THE JOURNAL OF PHYSICAL CHEMISTRY Letters

pubs.acs.org/JPCL

Oxygen Binding to Catalase-Peroxidase

Pietro Vidossich,*[,†,⊥] Xavi Carpena,[†] Peter C. Loewen,[#] Ignacio Fita,[†] and Carme Rovira*[,§]

[†]Laboratori de Simulació Computacional i Modelització, Parc Científic de Barcelona, Baldiri Reixac 10-12, 08028 Barcelona, Spain, [⊥]Institut de Química Teòrica i Computacional (IQTCUB), [†]Institute of Research in Biomedicine (IRB-Barcelona) and Institut de Biología Molecular (IBMB-CSIC), Parc Científic de Barcelona, Baldiri Reixac 10-12, 08028 Barcelona, Spain, [#]Department of Microbiology, University of Manitoba, Winnipeg, MB R3T 2N2, Canada, and [§]Institució Catalana de Recerca i Estudis Avançats (ICREA), Passeig Lluís Companys, 23, 08018 Barcelona, Spain

ABSTRACT By means of quantum mechanics/molecular mechanics calculations, we show that binding of dioxygen to the Fe^{III} enzyme catalase-peroxidase (KatG), responsible for activating the antitubercular drug isoniazid, is possible in the absence of an external reducing agent, thanks to the unique electronic properties of the active site Met-Tyr-Trp adduct. The calculations give support to recent experimental observations suggesting that KatG activates molecular oxygen and suggest that dioxygen activation may be achieved in other enzymes by inserting a residue with low ionization potential near the active site.

SECTION Biophysical Chemistry

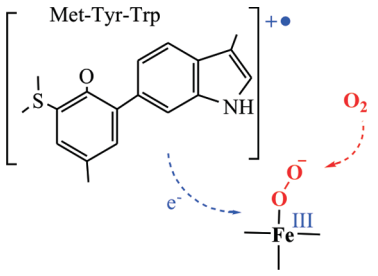

Selective oxidation reactions using dioxygen (O_2) as the oxidant are of enormous interest because of their economic and environmental impact.[1] Metalloenzymes are the natural catalysts of these reactions,[2] and extensive research in this area, particularly in the chemistry of heme[3] and nonheme iron enzymes,[4,5] has provided crucial mechanistic insights leading to the development of artificial catalysts.

Scheme 1 shows the main steps of dioxygen activation in heme enzymes, in which O_2 progresses, concomitant with an increase in the formal iron oxidation state, through the superoxoferric ↔ oxyferrous (Por-Fe^{III}—O_2^- ↔ Por-Fe^{II}—O_2, **A**), peroxoferric (Fe^{III}—OOH^+, **B**), and oxoferryl states ($Por^{+\bullet}$-Fe^{IV}═O, compound I, **C**, and Por-Fe^{IV}═O, compund II, **D**) in a series of electron (and proton)-transfer steps.[4] Diverse classes of heme enzymes differ in the nature of the reactive form (**A**, **B** or **C**, **D**) and in the type of reactivity that they exhibit. Obviously, a precondition for oxygen activation is that the active site be capable of binding oxygen. This is only possible in the Fe^{II} state. Therefore, enzymes which are Fe^{III} in their resting state (e.g., heme oxygenases such as cytochromes P450) require a one-electron reduction (first step in Scheme 1) by an electron donor (e.g., NADPH) to start the catalytic cycle.

An important class of heme enzymes are heme peroxidases, which enter Scheme 1 at **B** following reaction with hydrogen peroxide ($H_2O_2 = O_2 + 2e^- + 2H^+$), but they may also form the ferric superoxo species (**A**) following reaction of the ferric enzyme with a strong reducing agent under controlled conditions.[6] This leads to the question of whether or not peroxidases can activate oxygen under mild conditions. The direct reaction with oxygen would expand the reactive diversity of peroxidases, which normally oxidize substrates via one-electron abstraction rather than via oxygen atom transfer as in monooxygenases. Here, we demonstrate that catalase-peroxidases, a class of the peroxidase family, are indeed capable of O_2 activation and that this occurs *in the absence of an external reducing agent*.

Catalase-peroxidases (KatG's) are bifunctional enzymes in which catalase activity has been introduced within a peroxidase-like active site. X-ray crystallography revealed a unique triad of covalently linked side chains of distal side residues, Trp111, Tyr238, and Met264 (*Burkhoderia pseudomallei* KatG numbering throughout), the M—Y—W adduct, whose presence is required for catalase activity.[7] In *Mycobacterium tuberculosis,* KatG is responsible for the conversion of the pro-drug isoniazid into the active antitubercular agent isonicotinoyl-NAD.[7] The mechanism by which KatG activates INH has been the subject of several studies over the past decade. These studies revealed that (at least) two pathways are operative. The first goes through the peroxidatic activity of the protein. The second is a dioxygen-dependent pathway in which superoxide is produced.[8,9] This latter pathway is inhibited by cyanide,[10] an Fe^{III} ligand, suggesting that oxygen is activated via interaction with the heme. Further experimental evidence for O_2 activation by KatG comes from the crystal structures of KatG and its Ser324Thr variant, where a perhydroxy modification on the indole nitrogen of the distal Trp111[11−13] forms rapidly after shifting the crystal to a buffer with pH ≥ 6.5 and at lower pHs for the isoniazide-resistant Ser324Thr variant. One hypothesis for the origin of this modification is that a reactive dioxygen species is formed in the heme cavity of KatG[Fe^{III}].[12]

In previous work[14] on the electronic structure of KatG compound I (**C** in Scheme 1), we showed that the M—Y—W adduct may serve as an electron donor to the porphyrin cation

Received Date: November 23, 2010
Accepted Date: January 4, 2011

DOI: 10.1021/jz1015795 | *J. Phys. Chem. Lett.* **2011**, *2*, 196–200

Scheme 1. Main Steps for O_2 Activation by Heme Enzymes

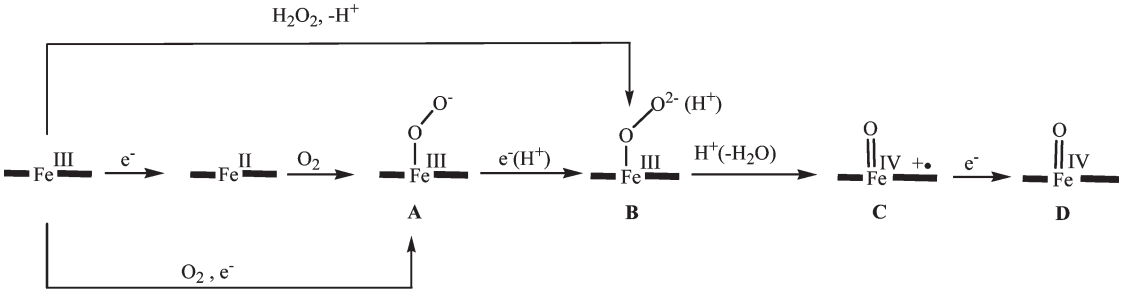

Table 1. Gas-Phase Ionization Energies[a]

system	IP (kcal/mol)
Por-Fe^{III}−O_2^-	136
Por-Fe^{II}−O_2^-	37
$M^+Y(O^-)W$	132
$M^+Y(OH)W$	218
Y^b	181
W^c	167

[a] Entries for Tyr and Trp are included for comparison. [b] Modeled by *p*-methylphenol. [c] Modeled by 3-methylindole.

radical, resulting in the formation of an oxoferryl/protein radical. The high electron-donor ability of the M−Y−W adduct suggests that it could also assist oxygen activation by donating one electron to the iron/oxygen moiety upon reaction of O_2 with the native enzyme (reaction 1).

$$\text{Por-Fe}^{III}\cdots O_2 + \text{M}-\text{Y}-\text{W} \rightarrow \text{Por-Fe}^{III}-O_2^- + \text{M}-\text{Y}-\text{W}^{+\bullet} \quad (1)$$

As a first approximation to this reaction (and to rationalize the subsequent results), we computed gas-phase ionization potentials (IPs) for the isolated fragments (Table 1) by means of density functional theory (see Supporting Information (SI) for full details). The IP of the adduct in its deprotonated form $[M^+Y(O^-)W]$ (132 kcal/mol) is lower than those of the individual tyrosine or tryptophan components and,[14] most importantly, is also lower than the IP of Por-$Fe^{III}\cdots O_2^-$ (136 kcal/mol). Consequently, this simple gas-phase model predicts that electron transfer from M^+−Y(O^-)−W to Por-$Fe^{III}\cdots O_2$ is favorable by a few kcal/mol. The presence in the adduct of the unprotonated tyrosine is strongly supported, even below pH 7, by the geometry of its interaction with Arg426.[15] The side chain of this arginine can occupy two alternative conformations depending on conditions, which was interpreted as a molecular switch to modulate the catalytic activity. As discussed in previous work,[14] the lower pK_a of the adduct tyrosine compared to a standard Tyr is due to the extended π system and the positively charged Met.

To improve the above description, hybrid quantum mechanics/molecular mechanics (QM/MM) calculations were performed to characterize the interaction of dioxygen with iron. We considered a large QM (DFT)[16] representation of the active site (~190 atoms, depending on the model) and a MM

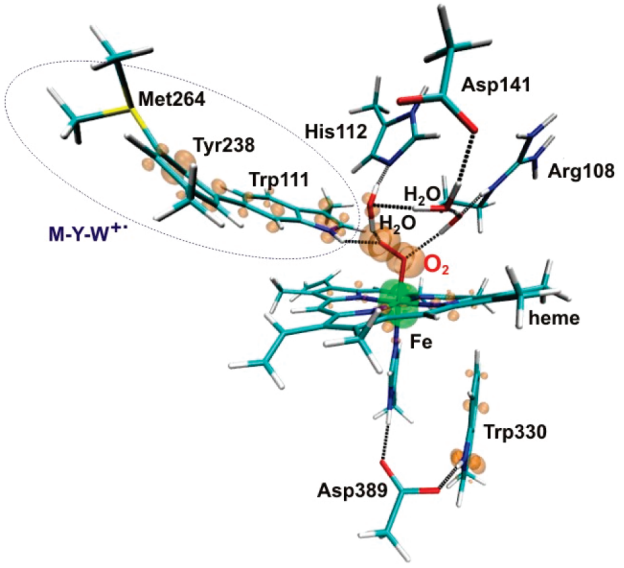

Figure 1. KatG[Fe^{III}−O_2^-, $M^+Y(O^•)W$] structure and electronic configuration. Structure obtained from QM/MM calculations of dioxygen bound to the ferric enzyme (KatG[Fe^{III}] + O_2, Table 2, left column). The QM region is shown in sticks together with the spin density isosurfaces at 0.005 (orange) and −0.005 (green) e $Å^{-3}$. The protein frame, solvent, and counterions are not shown for clarity.

Table 2. QM/MM Optimized Structures and Spin Densities

	KatG[Fe^{III}] + O_2	KatG[Fe^{III}] + O_2 + 1e^-
Distances (Å)		
Fe−O	1.91	1.92
O−O	1.35	1.30
ground state	doublet	singlet
Spin Distribution		
Fe	−1.00	−1.01
O_2	0.94	0.95
M−Y−W	0.52	0.01
porphyrin	0.27	0.04
Trp330	0.25	0.00

(AMBER) description of the protein and solvent environment (see SI for full details). The initial structures were taken from our previous work on KatG compound I, in which the structure

DOI: 10.1021/jz1015795 | *J. Phys. Chem. Lett.* 2011, *2*, 196–200

Scheme 2. Proposed Mechanism for O_2 Activation by KatG

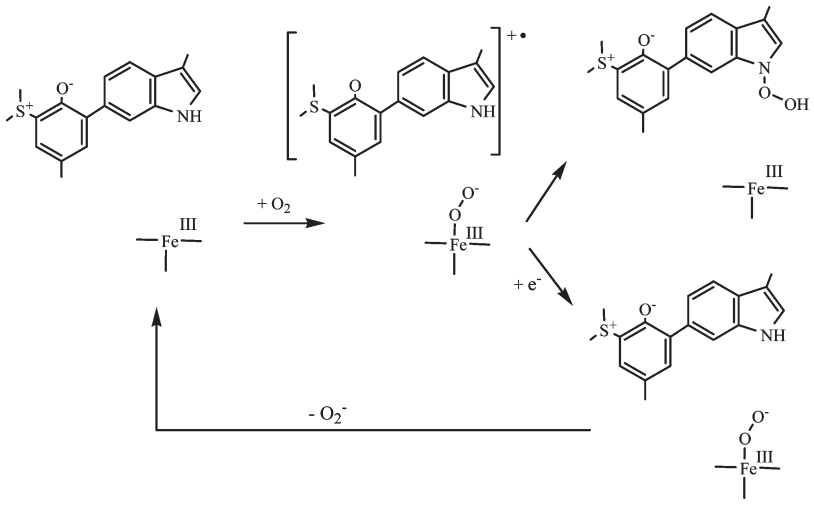

of KatG compound I was equilibrated with the AMBER force field and optimized within the QM/MM approximation. Five different scenarios were considered, (1) KatG[Fe^{III}] with bound O_2, (2) KatG[Fe^{III}] with unbound O_2, (3) KatG[Fe^{III}] with bound O_2 and deprotonated Trp111, (4) KatG[Fe^{III}] with bound O_2, with the addition of one electron, and (5) KatG[Fe^{III}] with no O_2 in the distal pocket (i.e., the resting state). The tyrosine of the M−Y−W adduct was considered as deprotonated in all cases. Structure optimization was performed by simulated annealing Car−Parrinello molecular dynamics using the QM/MM coupling scheme developed by Laio, VandeVondele, and Röthlisberger and the BP86 functional.[17] A short ab initio MD simulation (∼1 ps) was performed for the oxygen-bound enzyme to check that the structure corresponded to a stable state. To investigate all relevant spin states, we reoptimized the structure using the QM(B3LYP)/MM-(AMBER) implementation of NWCHEM.[18] The ground state of all systems was found to be in agreement with the experimental information available on KatG and similar heme proteins.[19]

The calculations reveal (Figure 1 and Table 2, left column) that O_2 does bind to the Fe^{III}, leading to a local electronic configuration around the iron atom that corresponds to an open-shell singlet, best described as a ferric superoxo ($Fe^{III}-O_2^-$) species.[20,21] The formation of this species requires the input of an electron which is supplied mainly by the adduct, with contributions from the proximal Trp330 and the porphyrin (Table 2, left column) leading to the species KatG-[$Fe^{III}-O_2^-$, ($M^+Y(O^\bullet)W$)]. This process is depicted in Scheme 2 (first step). As a control calculation, no spin density on the M−Y−W adduct is observed when a water molecule replaces O_2 at the iron site (see Figure S2 of the SI).

The calculations thus show that the $Fe^{III}-O_2^-$ species can be formed thanks to the electron-donor properties of the M−Y−W adduct. An estimate of the oxygen binding energy was obtained as the energy difference between the O_2-bound and the O_2-unbound situations (see Figure S2 of the SI for the O_2-unbound optimized structure, in which a water molecule occupies the sixth coordination position). The binding of O_2 in KatG turns out to be 11 kcal/mol. Excluding the distal M−Y−W adduct and the proximal W330 from the QM region[22] such that no electron transfer from surrounding residues is possible, oxygen binding requires >60 kcal/mol. While still unfavorable, the energy required for binding O_2 to KatG[Fe^{III}] is within reach of thermal fluctuations. Therefore, O_2 binding at the Fe^{III} center is possible due to the peculiar electronic properties of the active site, that is, the low ionization potential of the MY(O^-)W adduct.

The above results reveal that KatG[$Fe^{III}-O_2^-$, $M^+Y(O^\bullet)W$] corresponds to a stable minimum on the potential energy surface, which nevertheless is higher in energy than the unbound state and thus less populated at ambient conditions. This is consistent with EPR experiments that show that the five-coordinated high-spin ferric state is the most abundant species at pH 7.[12] However, being thermally accessible, the occurrence of KatG[$Fe^{III}-O_2^-$, $M^+Y(O^\bullet)W$] may explain previously reported experimental observations. First, the KatG-[$Fe^{III}-O_2^-$, $M^+Y(O^\bullet)W$] species contains two radicals in close proximity that are obvious precursors of the perhydroxy modification on the indole nitrogen of Trp111 (TrpN-OOH, Scheme 2 upper path) that forms at pH ≥ 6.5.[11−13] As shown in Figure S3 (SI), deprotonation of the TrpNH displaces the adduct spin density toward Trp111 ([$Fe^{III}-O_2^-$, $M^+Y(O^-)W-(N^\bullet)$], favoring coupling. Second, the KatG[$Fe^{III}-O_2^-$, $M^+Y-(O^\bullet)W$] species could act as a one-electron acceptor. Gas-phase calculations indicate that, of the two radical sites in the heme cavity (the adduct and the ferric superoxo moiety), $M^+Y(O^\bullet)-W \rightarrow M^+Y(O^-)W$ reduction is favored over Por-$Fe^{III}-O_2^- \rightarrow$ Por-$Fe^{II}-O_2^-$ reduction (−132 versus −37 kcal/mol; see Table 1). Indeed, QM/MM calculations show that addition of an electron to KatG[$Fe^{III}-O_2^-$, $M^+Y(O^\bullet)W$] leads to the formation of KatG[$Fe^{III}-O_2^-$, $M^+Y(O^-)W$], that is, the adduct radical is quenched (Table 2, right column, and Scheme 2, lower path). The resulting KatG[$Fe^{III}-O_2^-$] species is expected to decay, giving rise to superoxide,[23] and superoxide production is indeed observed when electron donors (e.g., isoniazid or NADH) are present.[10,24,25]

Recent spectroscopic measurements on KatG during catalatic turnover showed signals for an oxyferrous species and a

DOI: 10.1021/jz1015795 | J. Phys. Chem. Lett. 2011, 2, 196–200

protein-based radical, which was assigned to the M−Y−W adduct.[26,27] These features were interpreted as due to the formation of a KatG[$Fe^{III}-O_2^-$, $M^+Y(O^\bullet)W$] species.[26] The present calculations support the interpretation. However, we cannot say whether this species is directly involved in the last step of the catalatic reaction (Cpd I + H_2O_2 → Por-Fe^{III} + O_2 + H_2O)[27] or forms during the catalatic turnover[28] as a result of the interaction of the newly formed O_2 and the heme iron (given that the exothermicity of reaction 1, KatG[$Fe^{III}-O_2^-$, $M^+Y(O^\bullet)W$] may form to the level of being detectable).

In conclusion, we show that, thanks to the unique electronic properties of the M−Y−W adduct, KatG's are capable of binding O_2 in the absence of an external reducing agent. Our calculations provide a mechanism of dioxygen activation that, to the best of our knowledge, is new to heme peroxidase chemistry, although analogies may be found in the mode of action of other heme enzymes (e.g., cytochromes P450, cyt C oxidase).[29] The results support the interpretation of recent spectroscopic data,[26,27,30] offer an explanation for some crystallographic observations,[11−13] and provide mechanistic insight into the mode of activation of isoniazid.[8,9,30] Furthermore, the calculations suggest that dioxygen activation may be achieved in other enzymes by inserting a residue with low ionization potential near the active site. In the case of KatG's, one such structure, the Met-Tyr-Trp adduct, forms autocatalytically from standard aminoacids.

SUPPORTING INFORMATION AVAILABLE Computational details. Structures and spin density distributions for all species investigated. This material is available free of charge via the Internet at http://pubs.acs.org.

AUTHOR INFORMATION

Corresponding Author:

*To whom correspondence should be addressed. E-mail: vido@klingon.uab.es (P.V.); crovira@pcb.ub.es (C.R.).

ACKNOWLEDGMENT The authors thank the Ministerio de Ciencia e Innovación of Spain (MICINN, Grant FIS2008-03845), Generalitat de Catalunya (Grant 2009SGR-1309), NSERC, and the Canada Research Chair Program. We acknowledge the computer support, technical expertise, and assistance provided by the Barcelona Supercomputing Center — Centro Nacional de Supercomputación.

REFERENCES

(1) Centi, G.; Cavani, F.; Trifiro, F. *Selective Oxidation by Heterogeneous Catalysis*; Kluwer Academic/Plenum Publishers: New York, 2000.

(2) Messerschmidt, A.; Huber, R.; Wieghardt, K.; Poulos, T. *Handbook of Metalloproteins*; Wiley: Chichester, U.K., 2001.

(3) Matsui, T.; Unno, M.; Ikeda-Saito, M. Heme Oxygenase Reveals its Strategy for Catalyzing three Successive Oxygenation Reactions. *Acc. Chem. Res.* **2010,** *43*, 240–247.

(4) Mukherjee, A.; Cranswick, M. A.; Chakrabarti, M.; Paine, T. K.; Fujisawa, K.; Munck, E.; Que, L., Jr. Oxygen Activation at Mononuclear Nonheme Iron Centers: A Superoxo Perspective. *Inorg. Chem.* **2010,** *49*, 3618–3628.

(5) Que, L., Jr.; Ho, R. Y. Dioxygen Activation by Enzymes with Mononuclear Non-Heme Iron Active Sites. *Chem. Rev.* **1996,** *96*, 2607–2624.

(6) Zhao, X.; Yu, S.; Ranguelova, K.; Suarez, J.; Metlitsky, L.; Schelvis, J. P.; Magliozzo, R. S. Role of the Oxyferrous Heme Intermediate and Distal Side Adduct Radical in the Catalase Activity of *Mycobacterium tuberculosis* KatG Revealed by the W107F Mutant. *J. Biol. Chem.* **2009,** *284*, 7030–7037.

(7) Smulevich, G.; Jakopitsch, C.; Droghetti, E.; Obinger, C. Probing the Structure and Bifunctionality of Catalase-Peroxidase (KatG). *J. Inorg. Biochem.* **2006,** *100*, 568–585.

(8) Johnsson, K.; Schultz, P. G. Mechanistic Studies of the Oxidation of isoniazid by the Catalase-Peroxidase from *Mycobacterium tuberculosis*. *J. Am. Chem. Soc.* **1994,** *116*, 7425–7426.

(9) Wengenack, N. L.; Hoard, H. M.; Rusnak, F. Isoniazid Oxidation by *Mycobacterium tuberculosis* KatG: A Role for Superoxide which Correlates with Isoniazid Susceptibility. *J. Am. Chem. Soc.* **1999,** *121*, 9748–9749.

(10) Wiseman, B.; Carpena, X.; Feliz, M.; Donald, L. J.; Pons, M.; Fita, I.; Loewen, P. C. Isonicotinic Acid Hydrazide Conversion to Isonicotinyl-NAD by Catalase-Peroxidases. *J. Biol. Chem.* **2010,** *285*, 26662–26673.

(11) Deemagarn, T.; Carpena, X.; Singh, R.; Wiseman, B.; Fita, I.; Loewen, P. C. Structural Characterization of the Ser324Thr Variant of the Catalase-Peroxidase (KatG) from *Burkholderia pseudomallei*. *J. Mol. Biol.* **2005,** *345*, 21–28.

(12) Carpena, X.; Wiseman, B.; Deemagarn, T.; Herguedas, B.; Ivancich, A.; Singh, R.; Loewen, P. C.; Fita, I. Roles for Arg426 and Trp111 in the Modulation of NADH Oxidase Activity of the Catalase-Peroxidase KatG from *Burkholderia pseudomallei* Inferred from pH-induced Structural Changes. *Biochemistry* **2006,** *45*, 5171–5179.

(13) Zhao, X.; Yu, H.; Yu, S.; Wang, F.; Sacchettini, J. C.; Magliozzo, R. S. Hydrogen Peroxide-Mediated Isoniazid Activation Catalyzed by *Mycobacterium tuberculosis* Catalase-Peroxidase (KatG) and its S315T Mutant. *Biochemistry* **2006,** *45*, 4131–4140.

(14) Vidossich, P.; Alfonso-Prieto, M.; Carpena, X.; Loewen, P. C.; Fita, I.; Rovira, C. Versatility of the Electronic Structure of Compound I in Catalase-Peroxidases. *J. Am. Chem. Soc.* **2007,** *129*, 13436–13446.

(15) Carpena, X.; Wiseman, B.; Deemagarn, T.; Singh, R.; Switala, J.; Ivancich, A.; Fita, I.; Loewen, P. C. A Molecular Switch and Electronic Circuit Modulate Catalase Activity in Catalase-Peroxidases. *EMBO Rep.* **2005,** *6*, 1156–1162.

(16) Senn, H. M.; Thiel, W. QM/MM Methods for Biomolecular Systems. *Angew. Chem., Int. Ed.* **2009,** *48*, 1198–1229.

(17) Laio, A.; VandeVondele, J.; Rothlisberger, U. A Hamiltonian Electrostatic Coupling Scheme for Hybrid Car-Parrinello Molecular Dynamics Simulations. *J. Chem. Phys.* **2002,** *116*, 6941–6947.

(18) Kendall, R. A.; Apra, E.; Bernholdt, D. E.; Bylaska, E. J.; Dupuis, M.; Fann, G. I.; Harrison, R. J.; Ju, J. L.; Nichols, J. A.; Nieplocha, J.; Straatsma, T. P.; Windus, T. L.; Wong, A. T. High Performance Computational Chemistry: An Overview of NWChem, a Distributed Parallel Application. *Comput. Phys. Commun.* **2000,** *128*, 260–283.

(19) Sharma, K. D.; Andersson, L. A.; Loehr, T. M.; Terner, J.; Goff, H. M. Comparative Spectral Analysis of Mammalian, Fungal, and Bacterial Catalases. Resonance Raman Evidence for Iron-Tyrosinate Coordination. *J. Biol. Chem.* **1989,** *264*, 12772–12779.

(20) For the performance of QM(B3LYP)/MM to describe the FeO_2 bond in myoglobin, see, for instance: Chen, H.; Ikeda-Saito,

M.; Shaik, S. Nature of the Fe−O_2 Bonding in Oxy-Myoglobin: Effect of the Protein. *J. Am. Chem. Soc.* **2008,** *130*, 14778–14790.
(21) Unno, M.; Chen, H.; Kusama, S.; Shaik, S.; Ikeda-Saito, M. Structural Characterization of the Fleeting Ferric Peroxo Species in Myoglobin: Experiment and Theory. *J. Am. Chem. Soc.* **2007,** *129*, 13394–13395.
(22) This calculation corresponds to an ideal mutation in which the structural features of the M−Y−W adduct are maintained but its electronic structure is not allowed to change.
(23) Denisov, I. G.; Grinkova, Y. V.; Baas, B. J.; Sligar, S. G. The Ferrous-Dioxygen Intermediate in Human Cytochrome P450 3A4. Substrate Dependence of Formation and Decay Kinetics. *J. Biol. Chem.* **2006,** *281*, 23313–23318.
(24) Shoeb, H. A.; Bowman, B. U.; Ottolenghi, A. C.; Merola, A. J. Evidence for the Generation of Active Oxygen by Isoniazid Treatment of Extracts of *Mycobacterium tuberculosis* H37RA. *Antimicrob. Agents Chemother.* **1985,** *27*, 404–407.
(25) Singh, R.; Wiseman, B.; Deemagarn, T.; Donald, L. J.; Duckworth, H. W.; Carpena, X.; Fita, I.; Loewen, P. C. Catalase-Peroxidases (KatG) Exhibit NADH Oxidase Activity. *J. Biol. Chem.* **2004,** *279*, 43098–43106.
(26) Suarez, J.; Ranguelova, K.; Jarzecki, A. A.; Manzerova, J.; Krymov, V.; Zhao, X.; Yu, S.; Metlitsky, L.; Gerfen, G. J.; Magliozzo, R. S. An Oxyferrous Heme/Protein-Based Radical Intermediate is Catalytically Competent in the Catalase Reaction of *Mycobacterium tuberculosis* Catalase-Peroxidase (KatG). *J. Biol. Chem.* **2009,** *284*, 7017–7029.
(27) Zhao, X.; Suarez, J.; Khajo, A.; Yu, S.; Metlitsky, L.; Magliozzo, R. S. A Radical on the Met-Tyr-Trp Modification Required for Catalase Activity in Catalase-Peroxidase is Established by Isotopic Labeling and Site-Directed Mutagenesis. *J. Am. Chem. Soc.* **2010,** *132*, 8268–8269.
(28) Vlasits, J.; Jakopitsch, C.; Bernroitner, M.; Zamocky, M.; Furtmuller, P. G.; Obinger, C. Mechanisms of Catalase Activity of Heme Peroxidases. *Arch. Biochem. Biophys.* **2010,** *500*, 74–81.
(29) Shaik, S.; Cohen, S.; Wang, Y.; Chen, H.; Kumar, D.; Thiel, W. P450 enzymes: Their Structure, Reactivity, and Selectivity Modeled by QM/MM calculations. *Chem. Rev.* **2010,** *110*, 949–1017.
(30) Magliozzo, R. S.; Marcinkeviciene, J. A. Evidence for Isoniazid Oxidation by Oxyferrous Mycobacterial Catalase-Peroxidase. *J. Am. Chem. Soc.* **1996,** *118*, 11303–11304.

DOI: 10.1021/jz1015795 | *J. Phys. Chem. Lett.* **2011,** *2,* 196–200